

Activation Parameters of the Low Temperature Creep Controlling Mechanism in Martensitic Steels

M. Münch, R. Brandt

Abstract—Martensitic steels with an ultimate tensile strength beyond 2000 MPa are applied in the powertrain of vehicles due to their excellent fatigue strength and high creep resistance. However, the creep controlling mechanism in martensitic steels at ambient temperatures up to 423 K is not evident. The purpose of this study is to review the low temperature creep (LTC) behavior of martensitic steels at temperatures from 363 K to 523 K. Thus, the validity of a logarithmic creep law is reviewed and the stress and temperature dependence of the creep parameters α and β are revealed. Furthermore, creep tests are carried out, which include stepped changes in temperature or stress, respectively. On one hand, the change of the creep rate due to a temperature step provides information on the magnitude of the activation energy of the LTC controlling mechanism and on the other hand, the stress step approach provides information on the magnitude of the activation volume. The magnitude, the temperature dependency, and the stress dependency of both material specific activation parameters may deliver a significant contribution to the disclosure of the nature of the LTC rate controlling mechanism.

Keywords—Activation parameters, creep mechanisms, high strength steels, low temperature creep.

I. INTRODUCTION

LTC can be understood as time dependent plasticity that occurs at temperatures T , which are clearly below the melting temperature T_m , i.e. $T < 0.3 T_m$, and at stresses σ below the macroscopic yield strength $R_{p0.2}$. In contrast to high temperature creep, only primary creep is displayed and typical creep strains ϵ_{cr} are less than 1 % [1], [2]. The mechanism of plastic deformation at such low temperatures is identified as pure dislocation glide [3], [4]. Hence, the creep rate $\dot{\epsilon}_{cr}$ is generally described by the Orowan equation,

$$\dot{\epsilon}_{cr} = N \cdot A \cdot b \cdot f_0 \cdot \exp[-G/(k \cdot T)] \quad (1)$$

where N is the number of dislocation elements per unit volume contributing to creep, A the area swept out by a dislocation element after thermal activation, b the Burgers vector, f_0 an atomic frequency, G the activation energy and k the Boltzmann constant. The activation energy for this dislocation glide is strongly influenced by an applied stress τ or σ as well as an internal opposing stress σ_G , e.g. residual stresses. The stress dependent activation energy $G(\sigma)$ approximately reads,

M. Münch is with the University of Siegen, Siegen, ZIP 57074 Germany (Mathias Münch, phone: +49(0)271740-5050; e-mail: mathias.muench@uni-siegen.de).

R. Brandt is with the University of Siegen, Siegen, ZIP 57074 Germany (e-mail: Robert.brandt@uni-siegen.de).

$$G(\sigma) = G_0 - v \cdot (\sigma - \sigma_G) \text{ with } \sigma_G = h \cdot \epsilon_{cr} \quad (2)$$

where G_0 is a materials constant, v the activation volume and h a strain hardening coefficient [5]. Experimental studies reveal that the magnitude of creep strain ϵ_{cr} during LTC in high strength, martensitic steels is well described by a logarithmic creep law,

$$\epsilon_{cr} = \alpha \cdot \ln(\beta \cdot t + 1). \quad (3)$$

α and β are material specific parameters, which are functions of temperature T and stress σ . Creep tests have been conducted to review the creep behavior of martensitic steels at low temperatures in order to reveal the temperature and stress dependency of both parameters. However, the creep rate controlling mechanism in terms of (1) is still unclear. In order to shed light into it, temperature-step and stress-step tests have been conducted for the determination of both activation parameters G and v .

II. EXPERIMENTS

The materials testing have been conducted using wire rods of a martensitic steel 64SiCrV6. Its chemical composition is listed in Table I. The hot rolled wire rods have been shaved, recrystallized, cold drawn to a diameter of 3.7 mm, quenched and tempered by means of inductive heating prior to the LTC tests under tensile loading.

TABLE I
 CHEMICAL COMPOSITION OF THE STEEL (MASS%)

Material	C	Si	Mn	Cr	V	Ni	Fe
64SiCrV6	0.62	1.43	0.59	0.65	0.11	-	balance

The total lengths L_i of each wire are either $L_1 = 400$ mm for LTC testing and stress step testing or $L_2 = 170$ mm for temperature step testing, respectively. The samples for the temperature step test are additionally mounted with threaded fittings of a length of 42 mm. The LTC testing as well as the stress step testing have been done by means of a static materials testing machine Z 100 with a convection chamber. The engineering strain $\epsilon(t)$ has been measured at an initial length $l_{0,1} = 250$ mm by means of the extensometer multiXtens, which is classified to the accuracy class 0.5 in accordance to DIN EN ISO 9513. The temperature step tests are conducted by means of a Gleeble 3500 GTC machine, whereby $\epsilon(t)$ is measured at an initial length $l_{0,2} = 25$ mm with the extensometer MTS 634.12F_25. This is classified to the accuracy class 1 in accordance to DIN EN ISO 9513. The

LTC tests are performed either at a stress σ of 1400 MPa for the temperatures $T = 423\text{ K}$, 473 K and 523 K as well as at a temperature T of 423 K for stresses $\sigma = 800\text{ MPa}$, 1000 MPa, 1200 MPa and 1400 MPa. In order to ensure the complete heating of the samples, the convection chamber holds the temperature for 20 minutes before loading. The loading rate is 1 kN/s. A schematic illustration of the loading process is given by Fig. 1.

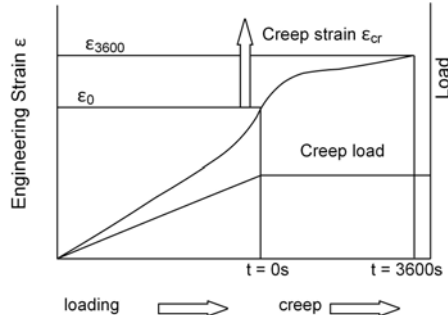


Fig. 1 Schematic illustration of the loading process

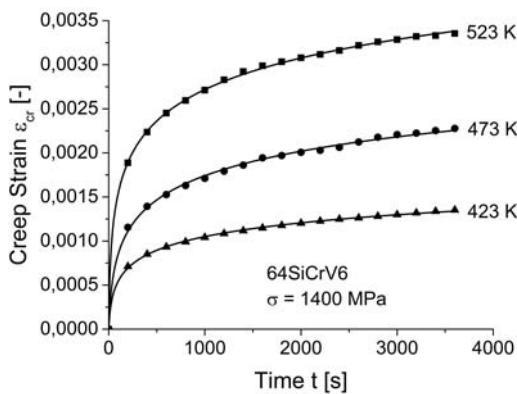
For the stress step test an initial stress $\sigma_0 = 1400\text{ MPa}$ is applied and subsequently increased by $\Delta\sigma = 20\text{ MPa}$ after one hour, respectively. Further stress step tests are performed at $\sigma_0 = 1400\text{ MPa}$, $\Delta\sigma = 100\text{ MPa}$ and at $\sigma_0 = 1600\text{ MPa}$, $\Delta\sigma = 20\text{ MPa}$ after only 30 minutes. All temperature step tests start at a temperature $T_0 = 363\text{ K}$ with temperature steps $\Delta T = 15\text{ K}$ at a rate $\dot{T} = 2\text{ K/s}$ and at a stress $\sigma = 1400\text{ MPa}$.

III. RESULTS

A. LTC Tests

Fig. 2 (a) reveals that the material exhibits a logarithmic creep behavior according to (3) with creep strains much lower than 1%. Even at a temperature of 523 K and at a stress $\sigma = 1400\text{ MPa}$ the creep strain achieves only a maximum value of about 0.3 %.

The logarithmic creep rate $\ln \dot{\epsilon}_{cr}$ displays a linearly descending behavior with ϵ_{cr} , so that only primary creep occurs. Fig. 3 shows the stress and temperature dependence of the material specific parameter α .



(a)

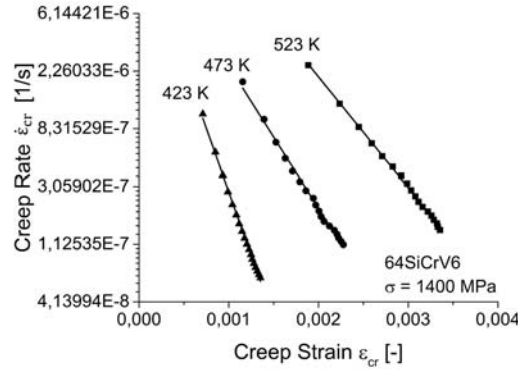
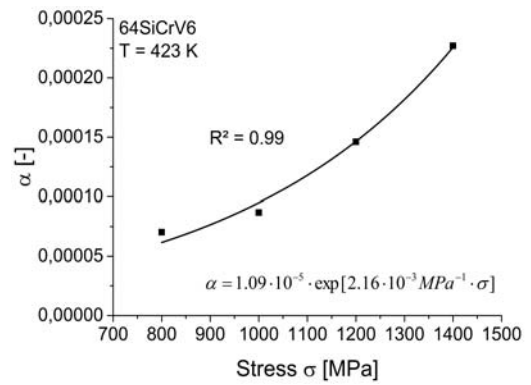
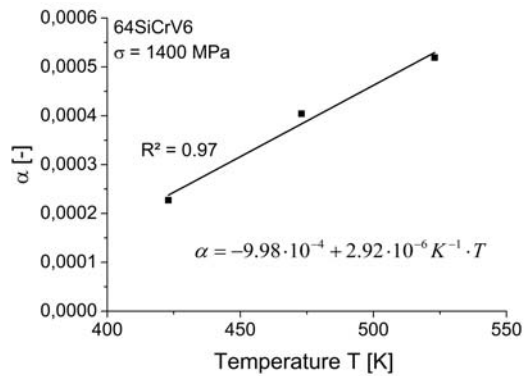


Fig. 2 (a) Creep Strain vs. time, (b) Creep rate vs. Creep Strain



(a)



(b)

Fig. 3 (a) Stress dependence of α , (b) Temperature dependence of α

It is obvious that α increases with stress and temperature, whereby the fitting line and the good coefficient of determination reveal an exponential stress and a linear temperature dependency. Fig. 4 illustrates the stress dependence of $\ln(\alpha \cdot \beta)$, which is well fitted by a linear fitting curve.

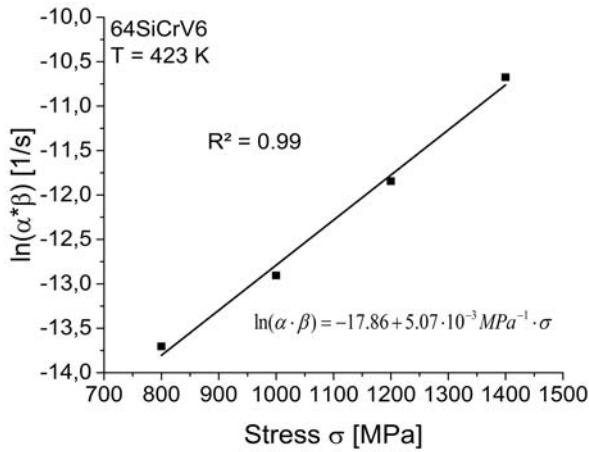


Fig. 4 Stress dependence of $\ln(\alpha \cdot \beta)$

B. Stress-Step-Tests

The creep strain during the incremental stress step tests is illustrated in Fig. 5, indicating the changes of stress $\Delta\sigma$ by a rapid increase in creep strain ϵ_{cr} . After the incremental step, the slope of the creep curve slightly increases.

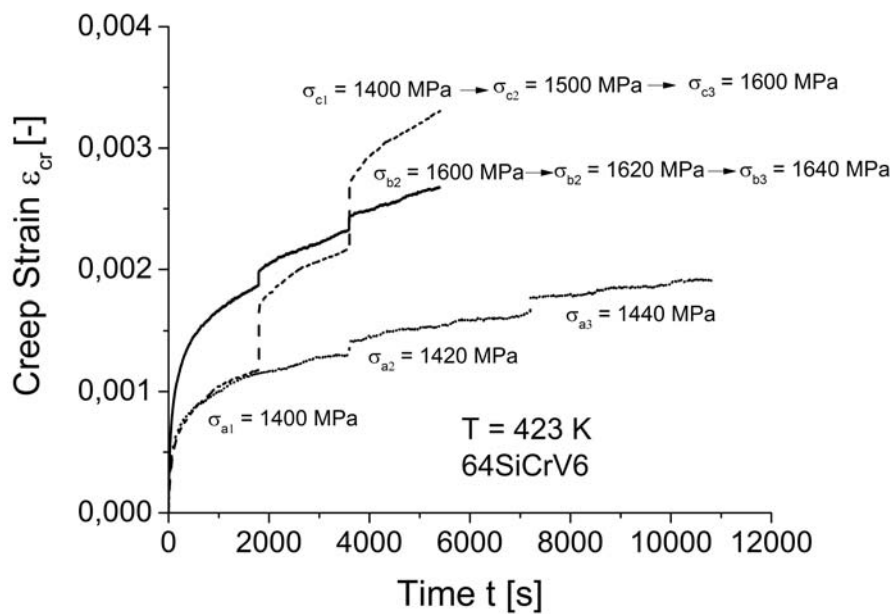


Fig. 5 Stress-step-tests with different variations in stress level, incremental step size and holding time for 64SiCrV6

The activation volume v is given by

$$v = -k \cdot T \cdot \ln(\dot{\epsilon}_{cr1} / \dot{\epsilon}_{cr2}) / \Delta\sigma \quad (4)$$

The determination of the creep rates $\dot{\epsilon}_{cr}$ is done by a fitting of the experimental values of the creep strains ϵ_{cr} and a subsequent derivation of the fitting function. The calculated activation volumes v are listed in Table II. These activation volumes can be expressed in terms of the Burgers vector b , whereby the most likely Burgers vector in martensitic steels is $a/2 [111]$ with the lattice constant $a = 0.2869 \text{ nm}$. The activation volumes are in a range of $4b^3 - 13b^3$.

C. Temperature-Step-Test

The creep strains of the temperature step test are shown in Fig. 6. The increase of the temperature leads to an abrupt increase in creep strain ϵ_{cr} . The slope of the creep curve after the temperature change is slightly increased, which is related to an increase in the creep rate $\dot{\epsilon}_{cr}$.

TABLE II
 ACTIVATION VOLUMES OF THE DIFFERENT TEST SERIES

Stress levels σ [MPa]	Activation volume v [$\times 10^{-28} \text{ m}^3$] / b^3	
	Stress Step 1	Stress Step 2
(a) 1400 \rightarrow 1420 \rightarrow 1440	1.17 / 8	1.15 / 8
(b) 1600 \rightarrow 1620 \rightarrow 1640	1.91 / 13	1.34 / 9
(c) 1400 \rightarrow 1500 \rightarrow 1600	0.61 / 4	1.24 / 8

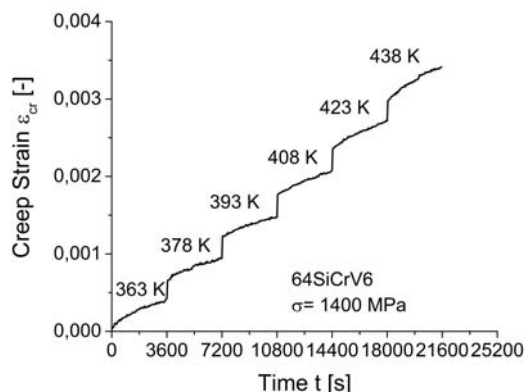


Fig. 6 Temperature-step-test with a step size of 15 K after one hour

Under the assumption that the structure is not changed during this time, the activation energy G then reads according to (1) [4], [6]

$$G = k \cdot \ln(\dot{\epsilon}_{cr1}/\dot{\epsilon}_{cr2}) / [(1/T_2) - (1/T_1)]. \quad (5)$$

The obtained values are listed in Table III,

Temperature T [K]	Activation energy G [kcal/mol]
363-378	26.0
378-393	25.6
393-408	25.8
408-423	19.8
423-438	26.8

IV. DISCUSSION

A. Stress and Temperature Dependence of the Material Specific Parameter α and β

The logarithmic law in (3) includes the material specific parameters α and β . Two types of theories, i.e. the exhaustion theory [7] and the strain hardening theory [8], are proposed to explain the logarithmic behavior of LTC in steels. Based on the strain hardening theory, α and β are obtained by comparing the Orowan equation (1) in combination with the strain hardening approach according to (2) to the logarithmic creep law in (3). This leads to

$$\alpha = k \cdot T / (v \cdot h) \quad (6)$$

and

$$\ln(\alpha \cdot \beta) = \ln(N \cdot A \cdot b \cdot f_0) - (G_0 - v\sigma) / kT. \quad (7)$$

Nevertheless, the experimental results show that α is well described by

$$\alpha = 1.09 \cdot 10^{-5} \cdot \exp(2.16 \cdot 10^{-3} MPa^{-1} \cdot \sigma), \quad (8)$$

i.e. a stress σ dependent equation. Since $k = 1.38 \cdot 10^{-23} J/K$, $T = 423 K$ and $v = 1.17 \cdot 10^{-28} m^3$ are constant, the

stress dependence may be caused by h . The calculated values of h according to (6) are listed in Table IV.

Stress σ [MPa]	Strain hardening coefficient h [GPa]
800	813
1000	528
1200	342
1400	223

Considering the temperature dependence of α , the experimental results are well fitted to

$$\alpha = -9.98 \cdot 10^{-4} + 2.92 \cdot 10^{-6} K^{-1} \cdot T, \quad (9)$$

i.e. a temperature T dependent equation. However, beside the linear temperature T dependence, a constant term occurs, which is not covered by (6). Thus, the temperature dependence of h can be determined for a stress $\sigma = 1400 MPa$ by (6). The obtained values are listed in Table V.

Temperature T [K]	h [GPa]
423	210
473	146
523	117

The strain hardening coefficient $h = h(\sigma, T)$ decreases with temperature, whereby h becomes infinite at $T = 342 K$. The magnitude of the strain hardening coefficient is by a factor 1000 higher than suggested by the second stage of strain hardening of single crystals. A more suitable description for the strain hardening of polycrystalline materials is given by,

$$\sigma(\epsilon_{cr}) \sim \epsilon_{cr}^n, \quad (10)$$

which may lead with a Taylor expansion approach at $\epsilon_{cr} = \epsilon_{cr,0}$ to a stress and temperature dependent strain hardening coefficient h^*

$$h^*(\sigma, T) = \partial \sigma / \partial \epsilon_{cr} |_{\epsilon_{cr} = \epsilon_{cr,0}}. \quad (11)$$

The stress dependence of $\ln(\alpha \cdot \beta)$ is well described by,

$$\ln(\alpha \cdot \beta) = -17.86 + 5.07 \cdot 10^{-3} MPa^{-1} \cdot \sigma \quad (12)$$

which reveals a linear increase with stress. This stress dependence is in good accordance to (7), which enables the following correlations:

$$\ln(N \cdot A \cdot b \cdot f_0) - G_0 / kT = -17.86 \quad (13)$$

$$(v / kT) = 5.07 \cdot 10^{-3} MPa^{-1}. \quad (14)$$

Under consideration of a temperature $T = 423 K$, the activation volume $v = 2.96 \cdot 10^{-29} m^3$. Furthermore, the

temperature dependence of β can be described by a modification of (7) to be

$$\beta(T) = NAbf_0/\alpha \cdot \exp[-(G_0 - v\sigma)/kT]. \quad (15)$$

B. Activation Parameters

The activation volumes determined by the stress step test (s. Table II) are in good agreement to the research group of Pandey [9]. However, the above value of v determined by (15) is 3 times below the activation volume established by the stress step test. The deviation might be explained by neglecting the stress dependence of h . This leads to the fact that the opposing internal stress σ_G has to be considered in the determination of the activation volume v

$$v = -k \cdot T \cdot \ln(\dot{\epsilon}_{cr1}/\dot{\epsilon}_{cr2})/(\Delta\sigma - \Delta\sigma_G). \quad (16)$$

Nevertheless, the magnitude of the activation volumes could clarify the mechanism in LTC for martensitic steels. According to [6], cross slip is accountable for LTC in martensitic steels. The activation energy determined by the temperature step tests reveals a temperature insensitivity, which agrees very well with [4].

V. CONCLUSION

In this study, LTC tests have been done to determine the stress and temperature dependence of the material specific parameter α and β . It is revealed that α increases exponentially with stress and linearly with temperature. However, these stress and temperature dependencies are not fully covered by means of the strain hardening theory approach. Therefore, stress and temperature dependencies of the strain hardening coefficient h are discussed, which are required for a more consistent characterization of LTC by means of the strain hardening theory approach.

ACKNOWLEDGMENT

We are grateful to Mubea Motorkomponenten GmbH for providing the high strength steel and funding to carry out these investigations.

REFERENCES

- [1] M. E. Kassner, K. Smith, "Low temperature creep plasticity," *Journal of Materials Research and Technology*, vol. 3, no. 3, pp. 280–288, 2014.
- [2] B. Alfredsson, I. Linares Arregui, J. Lai, "Low temperature creep in a high strength roller bearing steel," *Mechanics of Materials*, vol. 100, pp. 109–125, 2016.
- [3] A. Oehlert, A. Atrens, "Room temperature creep of high strength steels," *Acta metall. mater.*, vol. 42, no. 5, pp. 1493–1508, 1994.
- [4] R. W. Neu, H. Schitoglu, "Low-Temperature Creep of a Carburized Steel," *Metallurgical Transactions A*, vol. 23A, pp. 2619–2624, 1992.
- [5] P. R. Thornton, P. B. Hirsch, "The effect of stacking fault energy on low temperature creep in pure metals," *Philosophical Magazine*, 3:31, pp. 738–761, 2006.
- [6] H. Conrad, "Thermally activated deformation of metals," *Journal of metals*, pp. 582–588, 1964.
- [7] F. R. N. Nabarro, "Theory of crystal dislocations," Clarendon Press, Oxford, pp. 719–723, 1967.
- [8] E. Orowan, "The creep of metals," Glasgow, West Scotland Iron and Steel Institute, 1947.
- [9] K. K. Mani Pandey, Om Prakash, B. Bhattacharya, "Variation of

activation volume with temperature for Fe, Si, and Ge," *Materials Letters* 57, pp. 4319 – 4322, 2003.